

# Zero-Noise Extrapolation via Cyclic Permutations of Quantum Circuit Layouts

Zahar Sayapin,<sup>1,\*</sup> Daniil Rabinovich,<sup>2,1,3</sup> Nikita Korolev,<sup>2</sup> and Kirill Lakhmanskiy<sup>2</sup>

<sup>1</sup>*Skolkovo Institute of Science and Technology, Moscow, Russian Federation*

<sup>2</sup>*The Russian Quantum Center, Moscow, Russian Federation*

<sup>3</sup>*Moscow Institute of Physics and Technology, Moscow, Russian Federation*

(Dated: November 6, 2025)

Increasing the utility of currently available Noisy Intermediate-Scale Quantum (NISQ) devices requires developing efficient methods to mitigate hardware errors, taking into account the constraints of these devices such as medium number of qubits and limited connectivity between them. In this work we propose a novel Cyclic Layout Permutations based Zero Noise Extrapolation (CLP-ZNE) protocol for such a task. The method leverages the inherent non-uniformity of gate errors in NISQ hardware and exploits symmetries of quantum circuits with one-dimensional connectivity to extrapolate the expectation value, averaged over cyclic circuit layout permutations, to the level of zero noise. In contrast to the previous layout permutation based approaches, for  $n$  qubit circuit CLP-ZNE requires measurements of only  $O(n)$  different circuit layouts to reconstruct the noiseless expected value. When benchmarked against noise channels modeling the IBM Torino quantum computer, the method reduces a typical expectation value error by an order of magnitude, depending on the protocol specifications. By employing a noise model derived from real hardware specifications, including both depolarizing and  $T_1/T_2$  relaxation processes, these results give evidence for the applicability of CLP-ZNE to present-day NISQ processors.

## I. INTRODUCTION

Modern day quantum computing is limited to Noisy Intermediate Scale Quantum devices [1]. These devices are characterized by limited qubit counts, short coherence times, and imperfect gate operations, which together restrict the depth of quantum circuits that can be executed within a fixed error tolerance [2–5]. Achieving fully fault-tolerant quantum computation ultimately requires the development of quantum error correction [6], which currently still faces major experimental and resource challenges. Facing these limitations, alternative approaches are being actively developed.

Among these are variational quantum algorithms (VQAs)[7–10] which exhibit partial robustness to hardware noise, hardware-efficient methods leveraging native interactions [11–14], and a variety of quantum error mitigation (QEM) techniques [15–17]. These techniques seek to suppress the impact of noise without the heavy overheads of quantum error correction, relying instead on modified circuit executions or classical post-processing. Among these, zero-noise extrapolation (ZNE) [16, 18–23] stands out for its conceptual simplicity: it scales the effective noise strength in a controlled manner to estimate expectation values at multiple noise levels and extrapolate them to the zero-noise limit.

Existing noise-amplification strategies include, among others, circuit and gate folding [19–21], pulse stretching [16, 22], and exploiting spatial variations in gate fidelities via qubit layout permutations [23]. The permutation-based method takes advantage of non-uniform gate errors by executing the same logical circuit

across multiple qubit layouts, thereby effectively scaling the noise. While this approach has shown notable empirical error suppression, its provable guarantees hold only when all possible  $n!$  permutations of an  $n$ -qubit circuit are considered, rendering it computationally impractical. To address this, it is essential to devise a layout-selection strategy that reduces computational complexity and to generalize the method to realistic noise models.

In this work, we introduce the Cyclic Layout Permutation-based Zero-Noise Extrapolation (CLP-ZNE) protocol, which preserves the hardware-awareness of [23] while provably reducing computational overhead to  $O(n)$  for  $n$ -qubit circuits with linear or circular entangling gate topologies, and to  $O(n^2)$  for circuits with arbitrary connectivity. The method exploits circuit geometry to construct sets of cyclically permuted layouts: linear extrapolation of the corresponding noisy expectation values yields unbiased estimates of noiseless observables up to quadratic noise terms, even under multi-channel noise. The protocol requires no additional gates or non-native operations and can provably mitigate both unitary and non-unitary noise.

We numerically benchmark CLP-ZNE by estimating expected values of random instances of Sherrington-Kirkpatrick (SK) model, widely used as a mean field approach to spin glasses [24, 25], and of the transverse field Ising model minimized by a variational quantum circuit. In the numerical simulations we use the noise models derived from IBM Torino calibration data [26], exhibiting both depolarizing noise and  $T_1/T_2$  relaxation processes. In this setting, the protocol demonstrates a reduction of typical error for  $n = 12$  qubit random SK instances by a factor, ranging from 8 to 13 depending on the protocol adjustment. At the same time, for simplistic noise model, such as depolarization, the error suppression reaches orders of magnitude. The method also exhibits significant

\* Z.Sayapin@skoltech.ru

error suppression under strong noise, and simulations of the transverse-field Ising model further demonstrate its robustness against high level non-unital noise.

The manuscript is structured as follows. Section II formalizes the multi-channel noise model and derives the perturbative expansion for noisy expectation values. The CLP-ZNE protocol is presented and formalized in form of a theorem. Section IIIA reports numerical experiments emulating realistic device conditions and quantifies the mitigation performance for SK model Hamiltonian across different noise settings. Section IIIB is devoted to studying the performance of the protocol for strong levels of non-unital noise. Section IV concludes the paper.

## II. THEORY

In this section we introduce a general noise model used in the work to describe the decoherence processes in quantum circuits. Using the first-order perturbation theory, we derive expectation values of arbitrary observables under the considered noise model. It is demonstrated that by averaging the expected values over polynomially many cyclic permutations of quantum circuit layouts one can estimate the noiseless expectation exactly up to terms quadratic in the strength of the noise.

### A. Noise model

We consider a widely studied model, where the main source of noise comes in the form of gate imperfections [27, 28]. Let  $T$  be a set of all two-qubit gates in the considered circuit. Imperfect realization of a two-qubit gate  $g \in T$  is described by the channel  $G_N$  composed of the ideal gate  $g$  followed by a noisy channel  $\mathcal{N}_g$ ,

$$G_N = \mathcal{N}_g \circ g, \quad (1)$$

which acts as  $G_N[\rho] = \mathcal{N}_g[g\rho g^\dagger]$ . Here the channel  $\mathcal{N}_g$  is modeled as a linear combination of identity channel  $\mathcal{I}$  and a fixed set of  $d$  gate-independent noise operators  $\{\mathcal{E}_i\}_{i=1}^d$ ,

$$\mathcal{N}_g = \mathcal{I} + \sum_{i=1}^d q_g^i \mathcal{E}_i. \quad (2)$$

Here  $q_g^i$  represents the non-negative error rate associated with the gate  $g$  and error source  $\mathcal{E}_i$ . This form encompasses many standard models such as depolarizing, phase damping and general Pauli noise. Additionally, one can interpret (2) as a linear approximation of an arbitrary noise channel at the point of zero noise, allowing it to approximate other sources of errors, such as amplitude damping [29, 30]. It is important to emphasize that noise operators  $\mathcal{E}_i$  here represent physical quantum channels, shifted by an identity channel. We detail the

connection of these operators to quantum channels in the Appendix A. For the simplicity of the presentation, we assume that the single qubit gate errors can be neglected. Their effect, however, can be incorporated analogously, even if their noise channels differ from those of the entangling gates. Although single-qubit gates typically have higher fidelities, their contribution to the total error budget can become noticeable due to their relative abundance in a circuit. We quantify this effect in Section III.

After application of the noisy circuit the output state can be written as

$$\rho = \rho_0 + \sum_{s \neq 0} q_s \rho_s, \quad (3)$$

where  $q_s = \prod_{i=1}^d \prod_{g \in T} (q_g^i)^{s_g^i}$ . This expression represents a mixture of all possible state perturbations  $\rho_s$ , where the binary array  $s$  marks the noise operators that were applied after each quantum gate:  $s_g^i = 1$  ( $s_g^i = 0$ ) implies that the noise operator  $\mathcal{E}_i$  was (was not) applied after the gate  $g$  in the circuit for  $\rho_s$ . By construction, the matrices  $s$  satisfy the condition  $\sum_{i=1}^d s_g^i \leq 1 \forall g \in T$ , implying that only one of the noise operators  $\mathcal{E}_i$  might occur upon application of a single gate as specified in (2).

Assuming that the error rates  $q_g^i$  are small and subject to the condition  $(\max_{i,g} q_g^i)|T|d \ll 1$ , all quadratic and higher order terms in  $q_g^i$  could be neglected. This allows one to obtain the linear approximation for the noisy state  $\rho$  as

$$\rho = \rho_0 + \sum_{i=1}^d \sum_{g \in T} q_g^i \rho_g^i + O(q^2), \quad (4)$$

where  $\rho_g^i = \rho_s$  with  $s$  having only one non-zero entry,  $s_g^i = 1$ . Taking trace of (4) with an observable  $H$  we obtain the linear approximation of noisy expectation value  $E = \text{Tr } \rho H$ ,

$$E = E_0 + \sum_{i=1}^d \sum_{g \in T} q_g^i E_g^i + O(q^2), \quad (5)$$

where  $E_0 = \text{Tr } \rho_0 H$  is a noiseless expectation value and  $E_g^i = \text{Tr } \rho_g^i H$  are energy perturbations. The derived expression enables us to establish the CLP-ZNE protocol in the next section.

### B. Cyclic Layout Permutation based ZNE

To execute a quantum circuit on a quantum processor, the circuit must be transpiled and bound to a specific

layout, i.e. the circuit's abstract qubits should be injectively mapped to the physical qubits used for execution. For a given transpiled circuit and a qubit layout  $l$ , the expectation value (5) becomes

$$E_l = E_0 + \sum_{i=1}^d \sum_{g \in T} E_g^i q_{l(g)}^i + O(q^2), \quad (6)$$

where  $l(g)$  refers to a physical gate that would be used in place of an abstract gate  $g$  upon the choice of layout  $l$ . Notice that the perturbed energy terms  $E_g^i$  are typically not known and hard to compute, as they depend both on the noise channels and the unperturbed quantum state. Should they be known, the error mitigation would be straightforward, as  $E_0$  could easily be extracted from (6) after measuring  $E_l$ . The challenge here is to extract  $E_0$  having access only to the noisy expectation values  $E_l$  and gate error rates  $q_{l(g)}^i$ .

This can be achieved by utilizing a non-uniform distribution of gate infidelities in NISQ devices. As different layouts make use of distinct physical gates, each with its own fidelity, every layout  $l$  would produce a distinct expectation value. This fact, together with the expression (5)—though limited to the case of single channel—was used in [23] in order to establish a qubit permutation based ZNE protocol. This approach proposes to extrapolate the dependence of the expected value  $E_l$ , computed for random possible circuit layouts  $l \in L$ , on the circuit error sum  $\sum_{g \in T} q_{l(g)}^i$  to the level of zero noise, providing an approximation to the noiseless value.

The main drawback of the previously proposed protocol, however, was the lack of strategy for choosing the layouts: the utility of the protocol was rigorously proven only when all  $n!$  layouts were considered, creating immense computational overheads. A potentially less demanding approach could be to perform extrapolation over  $q_{l(g)}^i$  themselves, which would require computing energy for  $d|T| + 1$  circuit layouts, which can still be restrictive due to the factor  $|T|$ . We propose an alternative approach, based on averaging the expected values  $E_l$  in (6) over different circuit layouts  $l \in L$ , yielding

$$\langle E_l \rangle_{l \in L} = E_0 + \sum_{i=1}^d \sum_{g \in T} E_g^i \langle q_{l(g)}^i \rangle_{l \in L} + O(q^2). \quad (7)$$

To simplify the notation we further denote  $\langle q_g^i \rangle_L \equiv \langle q_{l(g)}^i \rangle_{l \in L}$  and  $\langle E \rangle_L \equiv \langle E_l \rangle_{l \in L}$ . Now if one considers a circuit layout  $L$  such that  $\forall i \in \{1, \dots, d\}$  the mean error rates  $\langle q_g^i \rangle_L$  do not depend on  $g$  for all  $g \in T$ , then the mean noisy expectation value becomes

$$\langle E \rangle_L = E_0 + \sum_{i=1}^d \Delta_i \left\langle \sum_{g \in T} q_g^i \right\rangle_L + O(q^2), \quad (8)$$

where  $\Delta_i = \left( \sum_{g \in T} E_g^i \right) / |T|$  is the average perturba-

tion originating from the error source  $\mathcal{E}_i$ . A simple form of equation (8) enables a straightforward error mitigation protocol. Given access to  $d + 1$  distinct sets of circuit layouts  $L$ , each characterized by different values of  $\left\langle \sum_{g \in T} q_g^i \right\rangle_L$ , one can perform a linear regression to extract the noiseless term  $E_0$ . The key step in this construction is to identify the sets of layouts that satisfy the gate independence of  $\langle q_g^i \rangle_L$ , ensuring the validity of (8).

This can be readily achieved for circuits with a one-dimensional topology, for example when the entangling gates form linear or circular structures—configurations that are frequently encountered in practical applications [31–33]. Given a circuit layout  $l$ , we identify a loop of  $m$  connected physical qubits on the device that includes all qubits and couplings used in the layout. We then define  $\mathcal{C}_m(l)$  as the set of  $m \geq n$  layouts obtained via cyclic permutations of the original layout  $l$  along this loop. Such loops can typically be identified in devices featuring two-dimensional connectivity, such as superconducting quantum processors [34, 35], or in fully connected architectures, as in trapped-ion quantum computers [36, 37]. In the following, whenever the specific loop size  $m$  is not essential for the discussion, the corresponding set of rotated layouts will be denoted simply by  $\mathcal{C}(l)$ .

**Theorem 1 (Cyclic Layout Permutation based Zero-Noise Extrapolation)**

Consider an  $n$ -qubit quantum circuit with local two-qubit interactions of one-dimensional topology. Assume there are  $d + 1$  layouts  $\{l_j\}_{j=1}^{d+1}$  which can be cyclically rotated over different loops of physical qubits. Then a linear extrapolation of the mean expected values  $\langle E \rangle_{\mathcal{C}(l_j)}$  with respect to the averaged total error rates  $\left\langle \sum_{g \in T} q_g^i \right\rangle_{\mathcal{C}(l_j)}$  to the level of zero noise provides an exact approximation  $E_{\text{mit}}$  of the noiseless expectation value up to terms, quadratic in  $q$ ,

$$E_{\text{mit}} = E_0 + O(q^2). \quad (9)$$

*Proof.* Due to the topology of the considered circuit, the mean noise strengths  $\langle q_g^i \rangle_{\mathcal{C}(l_j)}$ , obtained from averaging over the cyclic permutations of any layout  $l_j$ , would not depend on the gate  $g$ . Thus the expression (8) with  $L = \mathcal{C}(l_j)$  holds for every  $l_j$ . Introducing a design matrix  $X$  [38] with elements

$$X_{ij} = \begin{cases} 1, & j = 0 \\ \left\langle \sum_{g \in T} q_g^j \right\rangle_{\mathcal{C}(l_i)}, & 1 \leq j \leq d \end{cases} \quad (10)$$

equation (8) can be rewritten as  $\langle E \rangle_{\mathcal{C}(l_i)} = X_{i0} E_0 + \sum_{j=1}^d X_{ij} \Delta_j + O(q^2)$ . This dependence can be fit with a linear model which, after minimizing the square distance to the noisy expectation values, yields the mitigated ex-

pectation as  $E_{mit} = \sum_{j=0}^d X_{0j}^{-1} \langle E \rangle_{\mathcal{C}(l_j)}$ . Finially, we note that  $E_{mit} - E_0 = \sum_{j=0}^d X_{0j}^{-1} O(q^2) = O(q^2)$ , as the first row of  $X^{-1}$  remains finite for  $q \rightarrow 0$ , which finishes the proof.  $\square$

Several remarks should be made concerning the proof of Theorem 1. First, the linear and circular circuit topologies were considered only out of convenience, as their cyclic permutations automatically satisfy the gate independence of  $\langle q_g^i \rangle_L$ . The theorem, however, remains valid for arbitrary permutations, provided that this condition is fulfilled.

Second, the proof assumes that the matrix  $X$  is invertible, i.e., that the associated vectors of noise strengths are linearly independent. This condition is typically straightforward to satisfy in practice, given the inherently non-uniform fidelity distributions present in NISQ devices. In cases where the rows of  $X$  are linearly dependent, the requirement can still be relaxed: as long as  $X$  has full column rank, its inverse may be replaced with the Moore–Penrose pseudoinverse  $(X^\top X)^{-1} X^\top$ .

Finally, Theorem 1 also holds in the presence of single-qubit gate errors, even when the corresponding noisy channels differ from those of the two-qubit gates. The only additional requirement in this case is the inclusion of more layout permutations to ensure adequate averaging.

The conditions and proof of Theorem 1 thus establish the essential theoretical foundations of the proposed CLP-ZNE protocol. Below, we summarize its main steps for circuits with a one-dimensional topology, and graphically illustrate required steps in figure 1.

---

**Algorithm** CLP-ZNE (Cyclic Layout Permutation based Zero Noise Extrapolation)

---

**Input:** Quantum circuit with one-dimensional topology  $C$ , Observable  $H$

**Output:** Mitigated expected value of the observable  $E_{mit}$

- 1: Select  $d + 1$  layouts  $\{l_j\}_{j=1}^{d+1}$  of  $C$
- 2: **for**  $j = 1$  to  $d + 1$  **do**
- 3:   Generate a set of cyclically permuted layouts  $\mathcal{C}(l_j)$
- 4:   For each layout  $l' \in \mathcal{C}(l_j)$ , compute the expected value of observable  $E_{l'} = \text{Tr } \rho_{l'} H$ , where  $\rho_{l'}$  is the state prepared on a quantum computer by executing  $C$  using layout  $l'$
- 5:   Average the computed observables:  $\langle E \rangle_{\mathcal{C}(l_j)} = \text{average}(\{E_{l'} \mid l' \in \mathcal{C}(l_j)\})$
- 6:   Calculate average total error rates  $e_j^i = \left\langle \sum_{g \in T} q_g^i \right\rangle_{\mathcal{C}(l_j)}$
- 7: **end for**
- 8: Linearly extrapolate  $\langle E \rangle_{\mathcal{C}(l_j)}$  using average total error rates  $e_j^i$  to the zero-noise limit to obtain  $E_{mit}$
- 9: **return**  $E_{mit}$

---

Assuming all-to-all connectivity on the quantum hardware, the CPL-ZNE protocol applicability can be extended to quantum circuits with arbitrary entangling-gate topologies. In this setting, the averaging step of the protocol no longer yields a single gate-independent parameter per noise operator. Instead, it produces  $\lfloor \frac{n}{2} \rfloor$  distinct parameters per noise operator, each associated with entangling gates that correspond to chords of the  $n$ -qubit cycle. Consequently, one requires  $d \lfloor \frac{n}{2} \rfloor + 1$  distinct sets of  $n$  cyclically rotated qubit layouts, resulting in an overall complexity of  $O(n^2)$ .

While the proposed protocol can provably mitigate errors arising from gate imperfections, it does not account for other noise sources such as state preparation and measurement (SPAM) errors, and has to be used in conjunction with dedicated SPAM error mitigation techniques. Similarly, shot noise in measurement statistics would also adversely affect the protocol's performance. In Appendix B, we estimate its impact on the overall error mitigation efficiency.

### III. NUMERICAL VERIFICATION

In this section we numerically validate the developed CLP-ZNE protocol. We demonstrate the protocol performance for realistic noise models, derived from existing quantum hardware, establish the effect shot noise, and study protocol robustness against higher order noise terms in (3). All simulations are performed with the Qiskit framework [39], following the characteristics of the IBM Torino quantum computer [26] utilizing Heron architecture [40]. This device was a natural choice, as it features symmetric entangling CZ gates, assisting CLP-ZNE implementation. Other devices, i.e. those that use echoed cross-resonance entangling gates with predefined orientation, might restrict straightforward circuit rotations. The direction of such non-symmetric gates can effectively be reversed at the cost of additional single-qubit gates, which would contribute to the overall circuit infidelity.

To model the effect of the noise, we employ the Qiskit Aer framework, constructing a device-specific noise model using the `from_backend` method, which includes imperfections in both single- and two-qubit gates. Determining the gate error parameters  $q_g^i$  of the device, however, is generally a nontrivial task. Standard error characterization techniques include estimation of coherence times  $T_1, T_2$  and the average gate fidelity  $F_{avg}(G_N, g)$  by the means of randomized benchmarking [41, 42].

If the error is dominated by a single channel ( $d = 1$ ), the average infidelity  $1 - F_{avg}(G_N, g)$  of the gate  $g$  is directly proportional to the parameter  $q_g \equiv q_g^1$  within the linear approximation of  $G_N$ . In this case, the mitigation can be performed directly over the average infidelity, since the proportionality factor does not affect the extrapolation procedure. Interestingly, even in the

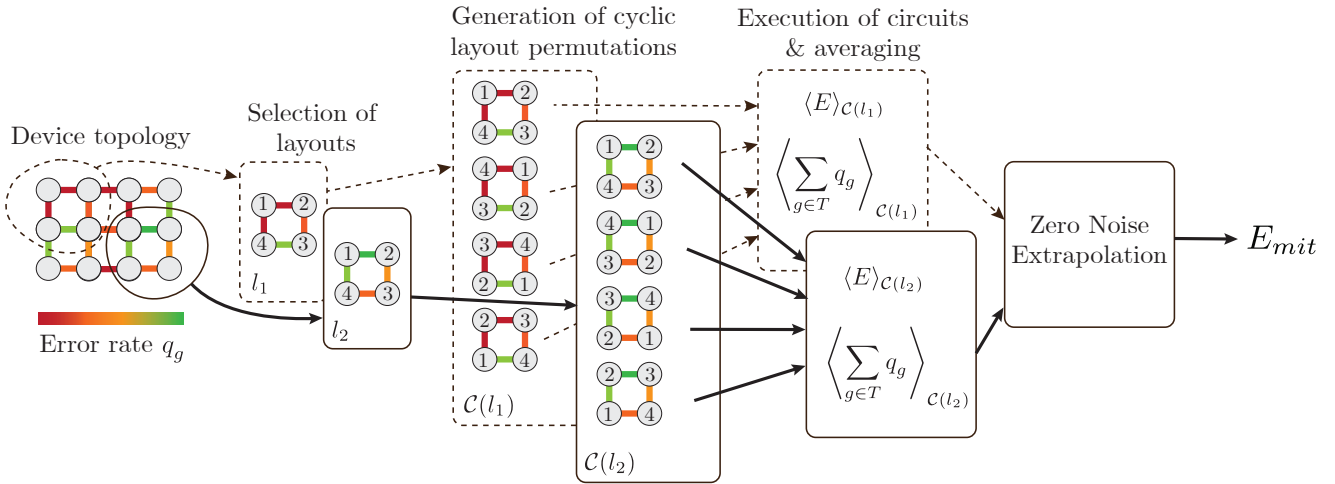


FIG. 1. **Schematic illustration of the proposed CLP-ZNE protocol for a four-qubit circuit with a single noise operator ( $d = 1$ ).** Circles represent physical qubits, while edges indicate available two-qubit couplings, color-coded according to their error rates. The procedure begins by selecting two circuit layouts,  $l_1$  and  $l_2$ , such that their total error rates are different. Abstract circuit qubits, labeled 1–4, are then mapped onto physical qubits according to each layout. Subsequently, cyclically permuted layout sets  $\mathcal{C}(l_1)$  and  $\mathcal{C}(l_2)$  are generated. For each layout within these sets, both the observable expectation value and the total error rate are computed and averaged over the respective sets. Finally, a linear regression is performed over the averaged values to extrapolate to the zero-noise limit, yielding the mitigated expectation value  $E_{\text{mit}}$ .

multichannel case ( $d > 1$ ), extrapolation over the gate infidelities still leads to a noticeable reduction in the error, as demonstrated below. Nevertheless, a complete implementation of the protocol would, in principle, require multidimensional extrapolation over all relevant error sources. In practice, a reasonable approximation of the dominant noise channels and their parameters can typically be inferred from the hardware specifications.

### A. Simulations for realistic noise

To demonstrate the ability of CLP-ZNE to suppress the errors in expectation values of measured observables, we compare the distributions of errors obtained from noisy circuit simulations before and after error mitigation. We generate an ensemble of 20 random 12-qubit circuits, each implementing a 3-layered `TwoLocal` ansatz [39] with circular connectivity, comprising single-qubit gates ( $R_x$  and  $R_z$ ) and CZ entangling gates. Each parameter in the circuit is initialized by sampling uniformly from the interval  $[0, 2\pi]$ . To ensure consistency in evaluation, all circuits are measured using an identical set of observables. As a benchmark, we consider 100 instances of the Sherrington–Kirkpatrick (SK) model with a homogeneous transverse field [24, 25].

$$H_{SK} = \frac{1}{\sqrt{n}} \sum_{i \neq j} J_{ij} Z_i Z_j + h \sum_{i=1}^n X_i, \quad (11)$$

where  $J_{ij} \sim \mathcal{N}(0, 1)$ ,  $Z$  and  $X$  are the Pauli operators. The transverse field strength  $h$  is set to 1. The full den-

sity matrix simulations are implemented to obtain noisy expected values of random SK instances in different circuit layouts, which are then used for extrapolation.

The results are summarized in figure 2, which demonstrates the distributions of errors of estimated expectation values  $E_l - E_0$ ,  $l \in \mathcal{C}(l_i)$ , obtained from cyclic permutations of several layouts  $l_i$ . It is compared to the distribution of errors of mitigated values  $E_{\text{mit}} - E_0$ , obtained from the CLP-ZNE protocol, conducted with respect to the total circuit infidelity. Figure 2a demonstrates the results for noise specification of IBM Torino device, exhibiting depolarization, and amplitude damping and dephasing, originating from  $T_1/T_2$  noise. It is seen that the CLP-ZNE protocol suppresses the typical scale of energy error by a factor of 8 when compared to the least noisy layouts  $\mathcal{C}_1 \equiv \mathcal{C}(l_1)$ , and provides even more dramatic improvement when compared to noisier circuit layouts  $\mathcal{C}_2 \equiv \mathcal{C}(l_2)$ . This confirms the applicability of the linear expansion (4) and the single channel  $d = 1$  approximation for CLP-ZNE realization on the considered NISQ processor. The latter is further verified by comparison of channels amplitudes: depolarization contributes  $\sim 0.13$  to the total circuit infidelity of 0.15 on cycle  $\mathcal{C}_1$  (see figure 3), while  $T_1/T_2$  processes only contribute the remaining 0.02. Apart from single channel approximation, the remaining width of the distribution is also attributed to the effect of single qubit gate errors. In their absence, the width of the distribution reduces by a factor of 13, providing even stronger error suppression. Moreover, in a simplified noise model in which all gate errors stem solely from depolarizing noise with an average gate infidelity of approximately  $10^{-3}$ , we observe a reduction in the characteristic error scale by several orders of magnitude.

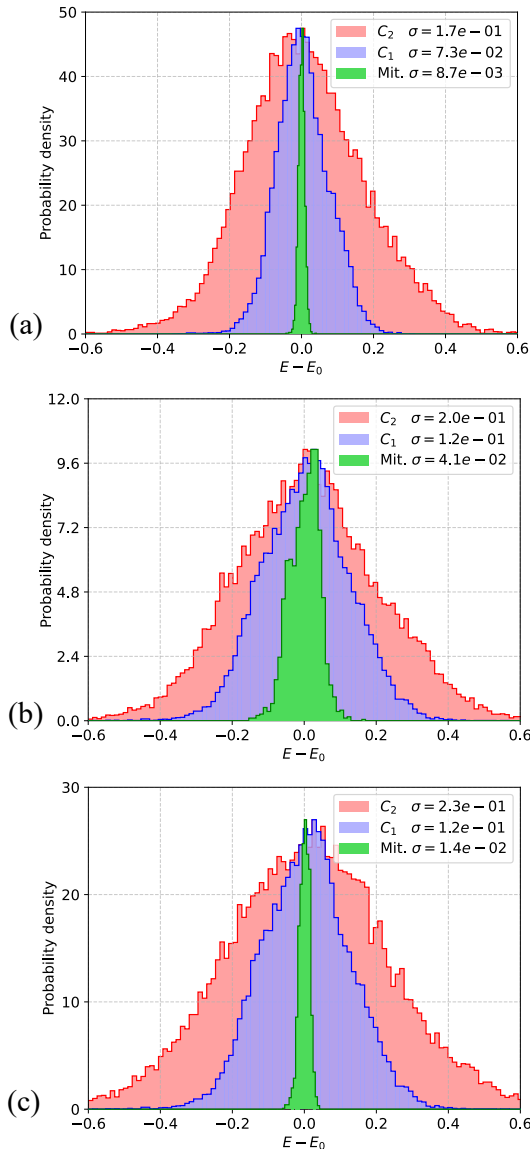


FIG. 2. The distributions of errors before and after the mitigation for (a) noise model derived from IBM Torino QPU calibration data, (b) analogous noise model, where each  $T_1, T_2$  is reduced by a factor of 10 and (c) multiparameter extrapolation over 4 cycles for the same noise settings as in case (b). The blue distribution is obtained from the cycle with the lowest total infidelity  $C_1$ , while the red is from a cycle with approximately double the infidelity. The values of  $\sigma$  represent standard deviations of the corresponding distributions. On each panel the distribution are normalize to the same height to facilitate visual comparison.

To test the versatility of the proposed protocol, we artificially reduce  $T_1, T_2$  times for every qubit by a factor of 10, and construct a new noise model with the least noisy cycle infidelity  $\sim 0.23$  with negligible input from depolarization. In this settings, due to comparable contributions from damping and pure dephasing channels, the quality of single parameter extrapolation degrades, as demon-

strated in figure 2b. Yet, the protocol still manages to reduce typical error by a factor of 3 compared to the least noisy circuit layouts. The performance of the protocol can be further improved in this case by performing a multidimensional extrapolation, as per protocol requirements, over  $d + 1 = 4$  circuit layouts, as shown in figure 2c: in this case CLP-ZNE suppresses the error by the factor of 9 compared to the cycle  $C_1$ . The noisiest cycle out of four considered is depicted as  $C_2$  here. The associated curves for the remaining two cycles would lie between the curves for  $C_1$  and  $C_2$  in figure 2c. Overall, these simulations demonstrate the CLP-ZNE protocol utility in various practically relevant conditions, expanding its applicability range compared to the analytical expectations.

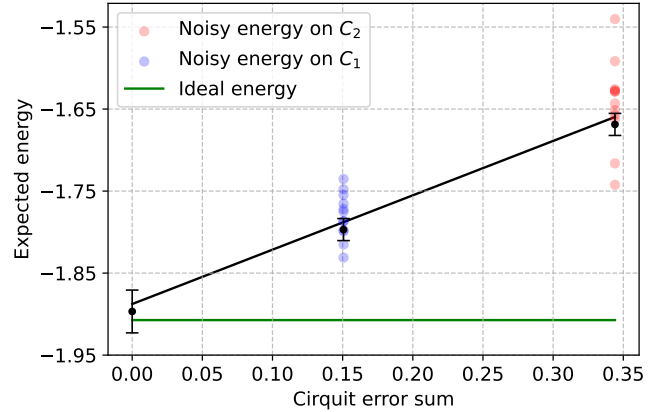


FIG. 3. A typical example of CLP-ZNE for one of the instances considered in figure 2 (a). The points are obtained from finite statistics of  $10^4$  shots used for every layout and measurement basis. The error bars on the noisy data denote the standard deviation, centered at the true average (black points). The error bars on the extrapolated value denote the standard deviation of  $E_{mit}$ , induced by the shot noise.

In figure 3 we exemplify a typical realization of CLP-ZNE protocol for the same settings as in figure 2a. For illustration, the simulation was conducted using finite statistics, using  $10^4$  shots for measuring (11) in X and Z bases for every circuit layout, demonstrating the stability of the mitigated value with respect to the finite statistics. Detailed analytical estimates on the effect of statistical error on the error mitigation efficiency is presented in Appendix B.

## B. Simulations for strong non-unital noise

In this section we investigate the role of high order terms in (4) by studying how the protocol performance degrades upon noise strength increase. We assume that the entangling two-qubit gates are subject only to the non-unital amplitude damping channels [43, 44], acting on both qubits separately, with associated non-uniform coherence times  $T_1$ . Note that in the case of amplitude

damping, even the form (2) only serves as a linear expansion of the channel, with  $\mathcal{E}$  originating from the derivative of the channel with respect to its strength. While, in theory, the protocol performance should not depend on the noise type, non-unital noise is known to nontrivially change the performance of quantum algorithms [45–47], making it a challenging testbed for error mitigation implementation. Ultimately, in this section we do not aim at replicating realistic device parameters, but test the robustness of the protocol against non-unital noise strength increase.

While the amplitude damping model can readily be built in terms of  $T_1$  time, here we implement it directly in terms of the channel strength  $\gamma = 1 - e^{-t/T_1}$ , ( $t$  being the gate duration) [44], which enters the channel via the Kraus operators

$$K_0 = \begin{pmatrix} 1 & 0 \\ 0 & \sqrt{1-\gamma} \end{pmatrix}, \quad K_1 = \begin{pmatrix} 0 & \sqrt{\gamma} \\ 0 & 0 \end{pmatrix}. \quad (12)$$

We assume this single-qubit error channel is applied after each entangling gate in the circuit, to both qubits with the associated strengths. To specify the problem, we focus on preparing the ground state of the cyclic transverse field Ising Hamiltonian

$$H_I = \sum_{j=1}^n Z_j Z_{j+1} + \sum_{j=1}^n X_i, \quad (13)$$

with  $Z_{n+1} \equiv Z_1$  by means of Variational Quantum Eigensolver (VQE) [9, 48] circuit. We use an  $n = 12$  qubit  $p = 4$  layer **TwoLocal** ansatz architecture [39], with each layer comprising a block of single-qubit  $R_Y(\theta)$  rotations followed by a cyclic nearest-neighbor entangling layer of CNOT gates. In the absence of noise the circuit optimization provides VQE energy within the energy error of 0.3 from the true ground state.

After the training, the circuit is subject to noise as explained above and CLP-ZNE is performed. For this we produce two sets of 12 values of  $\gamma_i^0$ , sampled uniformly from the range  $[0, 0.01]$ , to emulate the errors from two distinct qubit layouts. The CLP-ZNE protocol is then executed multiple times for noise strengths  $\gamma_i = \lambda \gamma_i^0$ . Such uniform noise scaling allows to directly assess protocol performance with respect to noise strength, without affecting the relative contributions of different channels. For each rescaling CLP-ZNE is then conducted with respect to the circuit error sum  $2p \sum_i \gamma_i$ , proportional to the sum of circuit gate infidelities. Note that although every entangling gate is now followed by two noisy channels, single parameter  $d = 1$  extrapolation is still justified due to the structure of the circuit, as can be confirmed with (8). The results of the simulations are demonstrated in figure 4. It is seen that while for the low noise strength the extrapolation accurately predicts the noiseless VQE, even within the gap of Hamiltonian  $H_I$ , the performance clearly degrades upon noise increase by deviating from the linear trend. For large circuit error sums the ex-

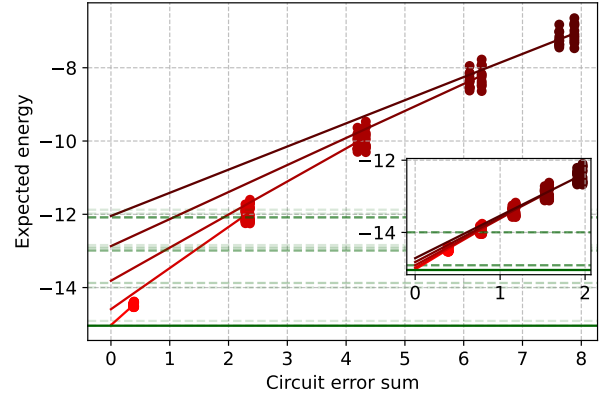


FIG. 4. CLP-ZNE realization for rescaled amplitude damping noise for 12 qubit VQE circuit. Different clusters of points depict noisy expectation values, with darker colors corresponding to noisier circuits. Solid horizontal line depicts the noiseless VQE energy, while the dashed lines are elevated by the energies of lowest excitations of  $H_I$ . Inset: same plot in the range of small circuit errors.

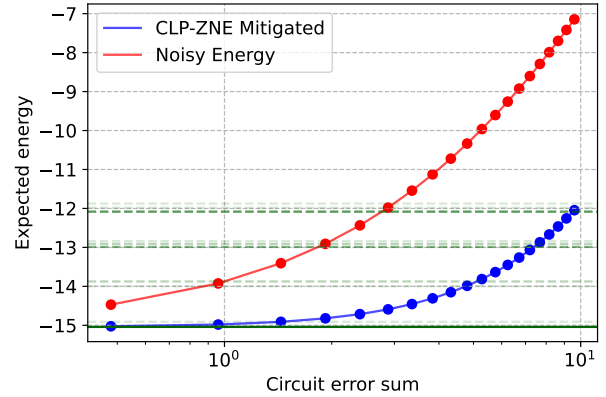


FIG. 5. Noisy and mitigated energies obtained for different circuit error sums  $2p \sum_i \gamma_i$  by rescaling the strengths  $\gamma_i$ . Solid horizontal line depict noiseless VQE energy, while the dashed lines are elevated by the energies of lowest excitations of  $H_I$ .

trapulation underestimates the noiseless energy, however, interestingly, the energy error still reduces by about a factor of 2.5. A direct comparison of the noisy and mitigated energy is demonstrated in figure 5. The mitigated expected value is seen to be within a spectral gap of  $H_I$  from the noiseless VQE for circuit error sum  $2p \sum \gamma_i \lesssim 1$ , comparable to the results of [23], yet with fewer circuit permutations required. The mitigated energy falls under the second gap (a more relevant energy scale, as the first gap separates states, degenerate in the thermodynamic limit) all the way to  $2p \sum \gamma_i \lesssim 5$ . Interestingly, while the effect of the error mitigation is seen even beyond this point, this behavior has been observed to be problem dependent. Overall, we conclude that CLP-ZNE protocol can successfully mitigate even moderately large non-unital noise.

#### IV. CONCLUSION

Executing quantum circuits on a quantum hardware requires finding a circuit layout into the topology of the device. Different layouts, while theoretically giving rise to the same unitary circuit, can strongly differ in practice due to the inhomogeneity of gate infidelities across the device. Thus, identifying a good layout in terms of connectivity and low circuit error is essential for modern day quantum computing. Yet, even the best circuit layouts can be quite noisy, which negatively affects the computation.

In the absence of error correction, an algorithmic or data post processing error mitigation methods can be used to assist the computation. A recent work [23] demonstrated that this inhomogeneity of errors in quantum computers can be exploited as a resource for error mitigation. Still, the proposed method was mostly empirical, lacking theoretical backing except in the extreme case, which required execution of  $n!$  circuits. Another limitation of the proposed method was an assumption of a single parameter noise model, that could not capture behavior of real world devices. Thus, this method required further development.

In this work we proposed a Cyclic Layout Permutation based Zero-Noise Extrapolation (CLP-ZNE) protocol, which utilizes the same idea of error inhomogeneity, but removes most of the previous protocol limitations. The idea is based on the extrapolation of the mean expected values, averaged across different circuit layouts, with respect to the sum of circuit errors. For circuits with linear or cyclic entangling topology, with gates subject to  $d$  distinct noisy channels, we proved that the noiseless ex-

pected value can be recovered exactly (up to the second order in the strength of the noise) by performing a multidimensional linear extrapolation of noisy expectation values obtained from  $n(d+1)$  cyclic circuit layouts. This provides a huge complexity reduction from the previously established  $n!$ , to just linear  $O(n)$  in terms of the number of qubits. Additionally, this gives a concrete recipe on how to choose the circuit layouts to perform exact extrapolation.

The analytical findings were further supported by numerically simulating the CLP-ZNE protocol for practically relevant hardware specifications of IBM Heron processor. We demonstrated that for the experimentally relevant parameters, a strong error reduction can be achieved by considering only  $2n$  layout rotations, and performing the extrapolation simply over the total circuit infidelity—the parameter readily accessible for many NISQ devices. Even when the contributions from different noisy channels were comparable, a usage of single channel approximation and extrapolation with respect to infidelity were observed to notably decrease errors in the measured observables. In this case, performing the multilinear extrapolation was seen to improve the accuracy of mitigated values even further. We also investigated the role of measurement statistics and bounded the associated extrapolation error. Finally, the applicability of the protocol was exemplified by demonstrating the ability to mitigate circuit errors for total noise strength  $\sim 1$  and beyond.

#### V. DATA AVAILABILITY

Data and code are available from the corresponding author on reasonable request.

---

[1] John Preskill. Quantum computing in the nisq era and beyond. *Quantum*, 2:79, 2018.

[2] Johannes Weidenfeller, Lucia C Valor, Julien Gacon, Caroline Tornow, Luciano Bello, Stefan Woerner, and Daniel J Egger. Scaling of the quantum approximate optimization algorithm on superconducting qubit based hardware. *Quantum*, 6:870, 2022.

[3] Alexander K Ratcliffe, Richard L Taylor, Joseph J Hope, and André RR Carvalho. Scaling trapped ion quantum computers using fast gates and microtraps. *Phys. Rev. Lett.*, 120(22):220501, 2018.

[4] Swathi S Hegde, Jingfu Zhang, and Dieter Suter. Toward the speed limit of high-fidelity two-qubit gates. *Phys. Rev. Lett.*, 128(23):230502, 2022.

[5] Adam R Mills, Charles R Guinn, Michael J Gullans, Anthony J Sigillito, Mayer M Feldman, Erik Nielsen, and Jason R Petta. Two-qubit silicon quantum processor with operation fidelity exceeding 99%. *Sci. Adv.*, 8(14):eabn5130, 2022.

[6] Peter W. Shor. Scheme for reducing decoherence in quantum computer memory. *Phys. Rev. A*, 52:R2493, 1995.

[7] Marco Cerezo, Andrew Arrasmith, Ryan Babbush, Simon C Benjamin, Suguru Endo, Keisuke Fujii, Jarrod R McClean, Kosuke Mitarai, Xiao Yuan, Lukasz Cincio, et al. Variational quantum algorithms. *Nat. Rev. Phys.*, 3(9):625–644, 2021.

[8] Jacob Biamonte. Universal variational quantum computation. *Phys. Rev. A*, 103(3):L030401, 2021.

[9] Jarrod R McClean, Jonathan Romero, Ryan Babbush, and Alán Aspuru-Guzik. The theory of variational hybrid quantum-classical algorithms. *New J. Phys.*, 18(2):023023, 2016.

[10] Daniil Rabinovich, Ernesto Campos, Soumik Adhikary, Ekaterina Pankovets, Dmitry Vinichenko, and Jacob Biamonte. Robustness of variational quantum algorithms against stochastic parameter perturbation. *Phys. Rev. A*, 109:042426, Apr 2024.

[11] Adrian Parra-Rodriguez, Pavel Lougovski, Lucas Lamata, Enrique Solano, and Mikel Sanz. Digital-analog quantum computation. *Physical Review A*, 101(2):022305, 2020.

[12] D. Rabinovich, S. Adhikary, E. Campos, V. Akshay, E. Anikin, R. Sengupta, O. Lakhmanskaya, K. Lakhman-skiy, and J. Biamonte. Ion-native variational ansatz for quantum approximate optimization. *Phys. Rev. A*, 106(3):032418, 2022.

[13] Georgii Paradezhenko, Daniil Rabinovich, Ernesto Campos, and Kirill Lakhmanskiy. Heuristic ansatz design for trainable ion-native digital-analog quantum circuits, 2025.

[14] J-Z Zhuang, Y-K Wu, and L-M Duan. Hardware-efficient variational quantum algorithm in a trapped-ion quantum computer. *Phys. Rev. A*, 110(6):062414, 2024.

[15] Suguru Endo, Zhenyu Cai, Simon C Benjamin, and Xiao Yuan. Hybrid quantum-classical algorithms and quantum error mitigation. *Journal of the Physical Society of Japan*, 90(3):032001, 2021.

[16] Kristan Temme, Sergey Bravyi, and Jay M. Gambetta. Error mitigation for short-depth quantum circuits. *Phys. Rev. Lett.*, 119:180509, 2017.

[17] Ying Li and Simon C Benjamin. Efficient variational quantum simulator incorporating active error minimization. *Physical Review X*, 7(2):021050, 2017.

[18] Suguru Endo, Simon C. Benjamin, and Ying Li. Practical quantum error mitigation for near-future applications. *Phys. Rev. X*, 8:031027, 2018.

[19] Tudor Giurgica-Tiron, Yousef Hindy, Ryan LaRose, Andrea Mari, and William J. Zeng. Digital zero noise extrapolation for quantum error mitigation. In *2020 IEEE International Conference on Quantum Computing and Engineering (QCE)*, pages 306–316, 2020.

[20] E. F. Dumitrescu, A. J. McCaskey, G. Hagen, G. R. Jansen, T. D. Morris, T. Papenbrock, R. C. Pooser, D. J. Dean, and P. Lougovski. Cloud Quantum Computing of an Atomic Nucleus. *Physical Review Letters*, 120(21), 2018.

[21] Andre He, Benjamin Nachman, Wibe A. de Jong, and Christian W. Bauer. Resource Efficient Zero Noise Extrapolation with Identity Insertions. *Physical Review A*, 102(1):012426, 2020.

[22] Abhinav Kandala, Kristan Temme, Antonio D. Córcoles, Antonio Mezzacapo, Jerry M. Chow, and Jay M. Gambetta. Error mitigation extends the computational reach of a noisy quantum processor. *Nature*, 567(7749):491–495, March 2019.

[23] Alexey Uvarov, Daniil Rabinovich, Olga Lakhmanskaya, Kirill Lakhmanskiy, Jacob Biamonte, and Soumik Adhikary. Mitigating quantum gate errors for variational eigensolvers using hardware-inspired zero-noise extrapolation. *Phys. Rev. A*, 110:012404, Jul 2024.

[24] Dmitry Panchenko. The Sherrington-Kirkpatrick model: an overview. *J. Stat. Phys.*, 149(2):362–383, 2012.

[25] David Sherrington and Scott Kirkpatrick. Solvable model of a spin-glass. *Phys. Rev. Lett.*, 35:1792–1796, Dec 1975.

[26] IBM Quantum. Fake provider: `fake_torino` — qiskit ibm runtime api documentation, 2025.

[27] William J. Huggins, Sam McArdle, Thomas E. O’Brien, Joonho Lee, Nicholas C. Rubin, Sergio Boixo, K. Birgitta Whaley, Ryan Babbush, and Jarrod R. McClean. Virtual distillation for quantum error mitigation. *Phys. Rev. X*, 11:041036, Nov 2021.

[28] Bálint Koczor. Exponential error suppression for near-term quantum devices. *Phys. Rev. X*, 11:031057, Sep 2021.

[29] Massimiliano F Sacchi and Tito Sacchi. Convex approximations of quantum channels. *Physical Review A*, 96(3):032311, 2017.

[30] Michael R Geller and Zhongyuan Zhou. Efficient error models for fault-tolerant architectures and the pauli twirling approximation. *Physical Review A—Atomic, Molecular, and Optical Physics*, 88(1):012314, 2013.

[31] Lorenzo Leone, Salvatore FE Oliviero, Lukasz Cincio, and Marco Cerezo. On the practical usefulness of the hardware efficient ansatz. *Quantum*, 8:1395, 2024.

[32] Abhinav Kandala, Antonio Mezzacapo, Kristan Temme, Maika Takita, Markus Brink, Jerry M Chow, and Jay M Gambetta. Hardware-efficient variational quantum eigensolver for small molecules and quantum magnets. *Nature*, 549(7671):242–246, 2017.

[33] Kouhei Nakaji and Naoki Yamamoto. Expressibility of the alternating layered ansatz for quantum computation. *Quantum*, 5:434, 2021.

[34] Sieu D. Ha, Edwin Acuna, Kate Raach, Zachery T. Bloom, Teresa L. Brecht, James M. Chappell, Maxwell D. Choi, Justin E. Christensen, Ian T. Counts, Dominic Daprano, J.P. Dodson, Kevin Eng, David J. Fialkow, Christina A. C. Garcia, Wonill Ha, Thomas R. B. Harris, nathan holman, Isaac Khalaf, Justine W. Matten, Christi A. Peterson, Clifford E. Plesha, Matthew J. Ruiz, Aaron Smith, Bryan J. Thomas, Samuel J. Whiteley, Thaddeus D. Ladd, Michael P. Jura, Matthew T. Rakher, and Matthew G. Borselli. Two-dimensional Si spin qubit arrays with multilevel interconnects. *PRX Quantum*, 6:030327, Aug 2025.

[35] Tian-Ming Li, Zheng-Hang Sun, Yun-Hao Shi, Zhen-Ting Bao, Yong-Yi Wang, Jia-Chi Zhang, Yu Liu, Cheng-Lin Deng, Yi-Han Yu, Zheng-He Liu, Chi-Tong Chen, Li Li, Hao Li, Hao-Tian Liu, Si-Yun Zhou, Zhen-Yu Peng, Yan-Jun Liu, Ziting Wang, Yue-Shan Xu, Kui Zhao, Yang He, Da'er Feng, Jia-Cheng Song, Cai-Ping Fang, Junrui Deng, Mingyu Xu, Yu-Tao Chen, Bozhen Zhou, Gui-Han Liang, Zhong-Cheng Xiang, Guangming Xue, Dongning Zheng, Kaixuan Huang, Zheng-An Wang, Haifeng Yu, Piotr Sierant, Kai Xu, and Heng Fan. Many-body delocalization with a two-dimensional 70-qubit superconducting quantum simulator, 2025.

[36] I. Pogorelov, T. Feldker, Ch. D. Marciniak, L. Postler, G. Jacob, O. Kriegelsteiner, V. Podlesnic, M. Meth, V. Negnevitsky, M. Stadler, B. Höfer, C. Wächter, K. Lakhmanskiy, R. Blatt, P. Schindler, and T. Monz. Compact ion-trap quantum computing demonstrator. *PRX Quantum*, 2:020343, Jun 2021.

[37] Colin D. Bruzewicz, John Chiaverini, Robert McConnell, and Jeremy M. Sage. Trapped-ion quantum computing: Progress and challenges. *Applied Physics Reviews*, 6(2), May 2019.

[38] Neil H. Timm. *Applied Multivariate Analysis*. Springer Texts in Statistics. Springer, New York, NY, 1 edition, 2002. Hardcover edition published 19 June 2002; soft-cover reprint ISBN 978-1-4419-2963-1 published 29 April 2013; eBook ISBN 978-0-387-22771-9 published 21 June 2007.

[39] Ali Javadi-Abhari, Matthew Treinish, Kevin Krsulich, Christopher J. Wood, Jake Lishman, Julien Gacon, Simon Martiel, Paul D. Nation, Lev S. Bishop, Andrew W. Cross, Blake R. Johnson, and Jay M. Gambetta. Quantum computing with qiskit, 2024.

- [40] Muhammad AbuGhanem. Ibm quantum computers: evolution, performance, and future directions. *The Journal of Supercomputing*, 81(5), April 2025.
- [41] E. Knill, D. Leibfried, R. Reichle, J. Britton, R. B. Blakestad, J. D. Jost, C. Langer, R. Ozeri, S. Seidelin, and D. J. Wineland. Randomized benchmarking of quantum gates. *Physical Review A*, 77(1), January 2008.
- [42] Ana Silva and Eliska Greplova. Hands-on introduction to randomized benchmarking. *SciPost Physics Lecture Notes*, July 2025.
- [43] Thomas Schuster, Chao Yin, Xun Gao, and Norman Y. Yao. A polynomial-time classical algorithm for noisy quantum circuits, 2024.
- [44] Vincent R. Pascuzzi, Andre He, Christian W. Bauer, Wibe A. de Jong, and Benjamin Nachman. Computationally efficient zero-noise extrapolation for quantum-gate-error mitigation. *Phys. Rev. A*, 105:042406, Apr 2022.
- [45] Bill Fefferman, Soumik Ghosh, Michael Gullans, Kohdai Kuroiwa, and Kunal Sharma. Effect of nonunital noise on random-circuit sampling. *PRX Quantum*, 5(3):030317, 2024.
- [46] Samson Wang, Piotr Czarnik, Andrew Arrasmith, Marco Cerezo, Lukasz Cincio, and Patrick J Coles. Can error mitigation improve trainability of noisy variational quantum algorithms? *Quantum*, 8:1287, 2024.
- [47] Enrico Fontana, Marco Cerezo, Andrew Arrasmith, Ivan Rungger, and Patrick J Coles. Non-trivial symmetries in quantum landscapes and their resilience to quantum noise. *Quantum*, 6:804, 2022.
- [48] Jules Tilly, Hongxiang Chen, Shuxiang Cao, Dario Picoczi, Kanav Setia, Ying Li, Edward Grant, Leonard Woessig, Ivan Rungger, George H. Booth, and Jonathan Tennyson. The variational quantum eigensolver: A review of methods and best practices. *Physics Reports*, 986:1–128, November 2022.

## Appendix A: Connection between noise operators and quantum channels

The noise model (2) encompasses different interpretations. First, it covers the case of a linear combination of different quantum channels  $\Phi_i$ ,

$$\mathcal{N}_g = (1 - \sum_{i=1}^d q_g^i) \mathcal{I} + \sum_{i=1}^d q_g^i \Phi_i. \quad (\text{A1})$$

Comparing it to (2) one immediately deduce the operators  $\mathcal{E}_i = \Phi_i - \mathcal{I}$ . Standard error models, such as depolarization, dephasing and general Pauli noise fall into this category. For example, depolarizing channel on  $n$ -qubits takes the form

$$\mathcal{E}(\rho) = (1 - p)\rho + \frac{p}{d^2} \sum_{i=0}^{d^2-1} P_i \rho P_i, \quad (\text{A2})$$

where  $d = 2^n$  is the dimension of the Hilbert space,  $p \in [0, 1 + \frac{1}{d^2-1}]$  is the depolarizing parameter,  $P_i$  are the  $n$ -qubit Pauli strings formed from the tensor products of

single-qubit Pauli operators:

$$P_i \in \{I, X, Y, Z\}^{\otimes n}.$$

Alternatively, consider a general quantum channel which is controlled by  $d$  gate dependent parameters,  $\mathcal{N}_g = \Phi(q_g^1, \dots, q_g^n)$ . In case of a weak noise, relevant for NISQ devices, this channel can be expanded, yielding a linear approximation

$$\mathcal{N}_g = \mathcal{E}(q_g^1, \dots, q_g^n) \approx \mathcal{I} + \sum_{i=1}^n q_g^i \mathcal{E}_i, \quad (\text{A3})$$

with the noise operators now given by  $\mathcal{E}_i = \Phi'_{q^i}(0, \dots, 0)$ . This case can be exemplified even further, if one considers a specific form of the channel,

$$\Phi = \Phi_1(q^1) \circ \dots \circ \Phi_d(q^d). \quad (\text{A4})$$

In this case  $\mathcal{E}_i = \Phi'_{q^i}(0, \dots, 0) = \Phi'_i(q^i = 0)$ . Moreover, the associated error rates admit simple physical interpretation: due to fidelity linearity,  $F_{avg}(\Phi_i) \approx 1 + q^i F_{avg}(\Phi'_i(0))$ , implying the proportionality between the error rate and gate infidelity

$$q^i \approx -\frac{1 - F_{avg}(\Phi_i)}{F_{avg}(\Phi'_i(0))} \propto 1 - F_{avg}(\Phi_i). \quad (\text{A5})$$

## Appendix B: Shot noise analysis

In practice, estimating expectation values on a quantum computer requires repeated measurements (or “shots”). Even in the absence of hardware noise, a finite number of shots introduces statistical uncertainty in the estimated expectation value—a phenomenon commonly referred to as shot noise. The empirical estimates of  $\langle E \rangle_j \equiv \langle E \rangle_{C_m(l_j)}$  used as inputs to the extrapolation procedure are therefore subject to this statistical error, which inevitably degrades the accuracy of the mitigated result  $E_{\text{mit}}$ .

To quantify this effect, we consider a regime where shot noise dominates the total error in  $E_{\text{mit}}$ , and systematic errors arising from first order perturbation approximation of noisy expected values are negligible. Under this assumption, the measured expectation values can be modeled as

$$\langle \hat{E} \rangle_j = E_0 + \sum_{i=1}^d \Delta_i \left\langle \sum_{g \in T} q_g^i \right\rangle_{C_m(l_j)} + \varepsilon_j, \quad (\text{B1})$$

where  $\varepsilon_j \sim \mathcal{N}(0, \text{Var}(\langle \hat{E} \rangle_j))$  represents the shot-noise-induced error for the  $j$ -th cycle, and  $\langle \hat{E} \rangle_j$  denotes the empirical estimate of  $\langle E \rangle_j$  obtained from finite sampling.

Performing a least-squares fit of the model in the equation (B1) yields a mitigated expectation value  $E_{\text{mit}}$

whose variance is given by

$$\text{Var}(E_{\text{mit}}) = [(X^\top X)^{-1} X^\top \Sigma X (X^\top X)^{-1}]_{00}, \quad (\text{B2})$$

where  $X$  is the design matrix (defined in equation (10)), and  $\Sigma = \text{diag}(\text{Var}(\langle \hat{E} \rangle_1), \dots, \text{Var}(\langle \hat{E} \rangle_{d+1}))$ .

To evaluate the shot-noise variance for a given circuit layout  $l$ , we decompose the Hamiltonian into  $C$  groups of mutually commuting Pauli terms:

$$H = \sum_{\alpha=1}^C H_\alpha, \quad (\text{B3})$$

where each  $H_\alpha$  contains only commuting Pauli strings and can be measured simultaneously. Assigning  $N_\alpha$  measurement shots to group  $\alpha$ , the variance of the energy estimator for circuit layout  $l$  is

$$\text{Var}(\hat{E}_l) = \sum_{\alpha=1}^C \frac{\text{Var}(H_\alpha)_l}{N_\alpha} = \sum_{\alpha=1}^C \frac{\langle H_\alpha^2 \rangle_l - \langle H_\alpha \rangle_l^2}{N_\alpha}, \quad (\text{B4})$$

where  $\langle \cdot \rangle_l$  denotes the expectation value with respect to the quantum state prepared by the circuit with layout  $l$ . Under the assumption of uniform shot allocation ( $N_\alpha = N/C$ ), this becomes

$$\text{Var}(\hat{E}_l) = \frac{C}{N} \sum_{\alpha=1}^C (\langle H_\alpha^2 \rangle_l - \langle H_\alpha \rangle_l^2). \quad (\text{B5})$$

The shot-noise variance for each empirical estimate  $\langle \hat{E} \rangle_j$  arises from averaging over  $m$  independent sets of

measurements. Specifically,

$$\text{Var}(\langle \hat{E} \rangle_j) = \frac{1}{m^2} \sum_{l \in \mathcal{C}_m(l_j)} \text{Var}(\hat{E}_l). \quad (\text{B6})$$

This layout-dependent expression clarifies that  $\text{Var}(\langle \hat{E} \rangle_j)$  may vary due to differences in the underlying quantum states—though, when circuit noise is weak, these variations are typically mild, thus we denote  $\text{Var}(\hat{E}_l) \approx \text{Var}(\varepsilon)$  for all  $l$ . This leads to the homoscedastic approximation:

$$\text{Var}(E_{\text{mit}}) = \frac{\text{Var}(\varepsilon)}{m} [(X^\top X)^{-1}]_{00}. \quad (\text{B7})$$

Combining equations (B7) and (B5), within homoscedastic approximation we obtain the standard deviation of the mitigated estimate  $\sigma_{E_{\text{mit}}} = \sqrt{\text{Var}(E_{\text{mit}})}$ ,

$$\sigma_{E_{\text{mit}}} = \sqrt{\frac{C [(X^\top X)^{-1}]_{00}}{mN} \sum_{\alpha=1}^C (\langle H_\alpha^2 \rangle - \langle H_\alpha \rangle^2)}. \quad (\text{B8})$$

For single error source extrapolation ( $d = 1$ ), this simplifies to

$$\sigma_{E_{\text{mit}}} = \sqrt{\frac{C (e_1^2 + e_2^2)}{mN (e_1 - e_2)^2} \sum_{\alpha=1}^C (\langle H_\alpha^2 \rangle - \langle H_\alpha \rangle^2)}, \quad (\text{B9})$$

where  $e_1 = \left\langle \sum_{g \in T} q_g^1 \right\rangle_{\mathcal{C}_m(l_1)}$  and  $e_2 = \left\langle \sum_{g \in T} q_g^1 \right\rangle_{\mathcal{C}_m(l_2)}$ .

These expressions show that the shot noise error in the mitigated result scales as  $1/\sqrt{mN}$ , consistent with known results from statistics. Consequently, to achieve a target error tolerance  $\epsilon$ , the total number of measurements must scale as  $O(1/\epsilon^2)$ .